Journal of Nuclear Materials 385 (2009) 212–215

Contents lists available at ScienceDirect

Journal of Nuclear Materials

journal homepage: www.elsevier.com/locate/jnucmat

The plutonium/hydrogen reaction: The pressure dependence of reaction initiation time

Gordon W. McGillivray *, John P. Knowles, Ian M. Findlay, Marina J. Dawes

AWE plc, Aldermaston, Berkshire RG7 4PR, United Kingdom

A B S T R A C T

The hydrogen pressure dependence of the initiation time (I_t) of the plutonium hydriding reaction has been determined over a hydrogen pressure range of 10–1000 mbar for plutonium covered in a dioxide over-layer. The data show that hydriding initiation time is inversely proportional to hydrogen pressure. This observation is consistent with a model of hydriding attack in which the dioxide over-layer acts as a diffusion barrier, controlling the flow of hydrogen to the oxide/metal interface. The low scatter and reproducibility of the experimental data set illustrate the importance of synthesising a reproducible oxide layer prior to determining this experimental parameter.

1. Introduction

The safe long term storage of plutonium metal requires an understanding of the metal's susceptibility to hydriding corrosion [1–4]. When plutonium is exposed to a hydrogen containing atmosphere, the course of the reaction follows the general form set out in Fig. 1; a process which can be described by four sequential steps. Step 1 – Induction: The plutonium is exposed to a hydrogen pressure and there follows a period during which no hydrogen consumption, as determined by either pressure drop or hydride formation, is observed. Step 2 – Nucleation or acceleration: Hydride spots are observed forming on the metal surface; with the time of formation of the first spot termed the induction time or initiation time (I_t). The rate accelerates as spots are formed at a rate termed the nucleation rate (N_r) and the size of individual spots increases, thereby increasing the reacting surface area and observed rate. Step 3 – Bulk hydriding: The coupon surface is now totally covered by hydride, which advances into the metal as a coherent hydriding reaction front at a rate determined by hydrogen pressure and temperature. The observed rate declines slowly as the reacting area decreases due to consumption of the metal; the so-called 'contracting envelope' effect identified by Bloch and Mintz [5] to explain the observed bulk hydriding behaviour of uranium. Step 4 – Termination: One of the reactants (in most controlled experiments, the metal) is consumed, and the observed rate falls to zero.

The induction and nucleation phases can be rationalised in terms of a diffusion barrier model, in which hydrogen species have to diffuse through the oxide layer which always covers the metal before reaction with the metal itself. If the flux of hydrogen species through the oxide exceeds the flux of hydrogen species into the metal, a concentration of hydrogen will develop at the oxide/metal interface. When this concentration reaches the solubility limit for hydrogen in the metal, hydride will precipitate. For an oxide layer with isotropic hydrogen transport properties, hydriding will initiate first at those regions where the oxide is thinnest. The observed hydriding attack pattern (Fig. 2) is consistent with a protective oxide of variable thickness, the variation being due to the differing oxidation rates of randomly oriented metal crystallites in the near-surface region. This model, currently only qualitative, is entirely analogous to the model developed by Bloch et al. [6–9] and Glascott [10] to explain the observed hydriding behaviour of massive uranium.

For plutonium, a predictive model of hydriding behaviour requires quantification of the parameters which affect hydriding initiation. Previous studies into plutonium hydriding kinetics have, for the most part, concentrated on characterising bulk hydriding behaviour [11–16] and those which have referred to hydriding initiation time explicitly [17–19] have not quantified either precise values or reaction conditions. This study represents an initial step toward the quantification of plutonium hydriding initiation time as a function of relevant reaction parameters. Specifically, this study used a controlled synthetic route to grow a reproducible oxide layer on clean plutonium surfaces, allowing hydriding initiation time to be quantified as a function of a single variable; namely hydrogen pressure.

2. Experimental

2.1. Coupon preparation and oxide growth

All experimental work was conducted in a nitrogen purged glovebox, which had a typical moisture level of 2 ppm. Coupons

* Corresponding author. Tel.: +44 118 9824860.
E-mail address: Gordon.McGillivray@awe.co.uk (G.W. McGillivray).

0022-3115/$ - see front matter Crown Copyright © 2008 Published by Elsevier B.V. All rights reserved.
doi:10.1016/j.jnucmat.2008.09.046

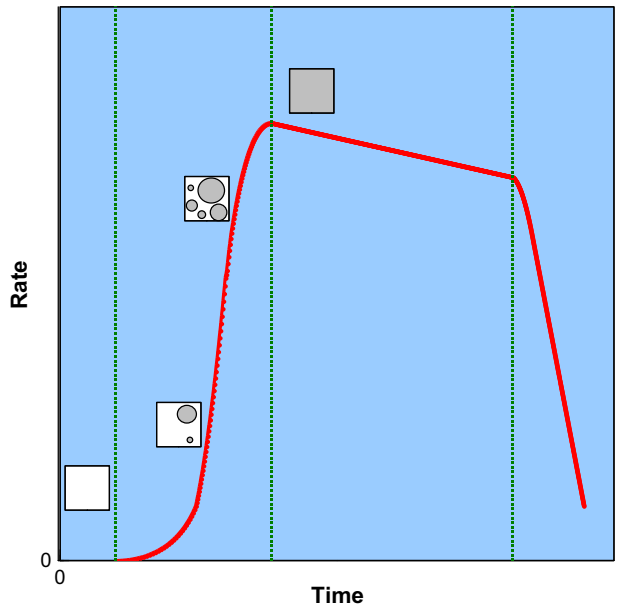

Fig. 1. Plot showing the general form of an observed rate vs. time curve for the plutonium hydriding reaction. The hatched vertical lines delineate the four sequential steps which describe the reaction profile: (1) induction, (2) nucleation or acceleration, (3) bulk hydriding, and (4) termination.

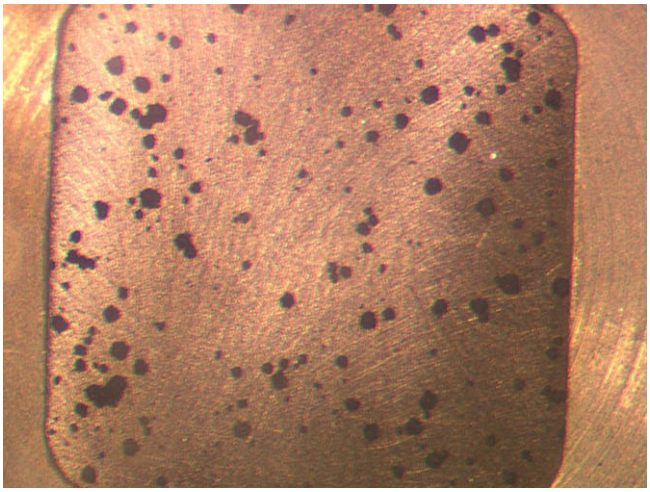

Fig. 2. Typical hydriding attack pattern. This morphology of hydriding attack can be rationalised in terms of hydrogen diffusion through an overlying oxide layer of variable thickness. In analysing a series of such images to determine initiation time, it is assumed that hydriding spot radial growth rate is constant and that consequently the largest spot was the first to form.

measuring 12 × 12 × 2 mm were polished on 1 face with 400 grit alumina pads using dry ethanol as a lubricant. The coupons were then washed with dry ethanol and allowed to evaporate to dryness. Coupons were placed on a hot stage and held in position with a stainless steel mask, which gripped the coupon at its edges. The stage was then sealed into a 300 cm^3 visual reaction cell; the coupon being positioned under a 16 mm sapphire window. The entire gas handling line was of stainless steel construction, and was pumped using turbo pumps which achieved base vacuum (within the cell) of 1×10^{-7} mbar.

Once a coupon was located within the reaction cell and system base vacuum was achieved, an oxide layer was grown on the coupon. The coupon was heated to 423 K under dynamic vacuum. Once temperature stability was achieved, 10 mbar of oxygen was introduced. The coupon was held under oxygen, at 423 K for 15 min. The oxygen was then evacuated, and the cell held at 423 K for a further 15 min. The reaction cell was then allowed to cool to 298 K under dynamic vacuum prior to the introduction of hydrogen. The cooling phase from 423 to 298 K took place overnight.

2.2. Materials used

Hydrogen gas was generated electrolytically by a Whatmans H2-1200 which generated hydrogen of 99.9999% purity. This gas stream was purified further by storage on a $LaNi_5$ bed. The gas was transferred to a storage volume adjacent to the reaction cell, and was subsequently delivered into the reaction cell via an MKS pressure controller. All pressure measurement was by MKS Baratrons. All experiments were conducted under constant pressure conditions. The plutonium used was cast, gallium stabilised δ-phase alloy. Major impurities were americium 400 ppm (wt) and carbon 200 ppm (wt). Minor metallic impurities (Ni + Fe + Al + Si) totalled 1100 ppm (wt).

2.3. Oxide characterisation

The oxide was characterised by X-ray diffraction (XRD) using a Siemens D5000 diffractometer employing Cu–Kα radiation (1.54056 Å), an operating voltage of 30 kV and a current of 40 mA. The diffractometer was housed within a dry (<10 ppm water) nitrogen glovebox. All measurements were performed at ambient temperature, and diffraction patterns were collected over a 2Θ range of 20–90°, with a step size of 0.02° 2Θ and at a rate of 20 s per step. XRD showed that the oxide layer was predominantly plutonium dioxide, with a weak signal indicating the presence of some α-sesquioxide. This observation is consistent with the fact that plutonium's oxide over-layer has a layered duplex structure, with PuO_2 at the surface/gas interface and Pu_2O_3 at the metal/oxide interface [20,21]. It was not possible in this study to either quantify oxide thickness or confirm that the outer oxide surface was dioxide, although this latter limitation will be addressed in future work when an Auger capability is available.

2.4. Data capture and analysis

Initiation time (I_t) was determined by analysing static images acquired during the course of the reaction. Coincident with the introduction of hydrogen into the reaction cell, an image capture system started taking images of the coupon surface. Images were taken at regular, pre-determined intervals during the entirety of the hydriding phase. Post-experiment analysis of these images used Image ProPlus™ image analysis software to determine the time to formation of the first hydride spot (the initiation or induction time I_t). Fig. 3 shows a sequence of images from a typical experiment. Reaction was terminated by evacuation of the hydrogen.

3. Results

A series of experiments were conducted over the hydrogen pressure range 10–1000 mbar, using coupons which had an oxide layer grown by the method described above. Fig. 4 shows a log vs. log plot of initiation time (I_t) vs. applied hydrogen pressure (P) for the entire data set. A least squares fit to the data yielded a slope of −0.91. This is sufficiently close to a value of −1 to indicate that hydriding initiation time varies inversely with hydrogen pres-

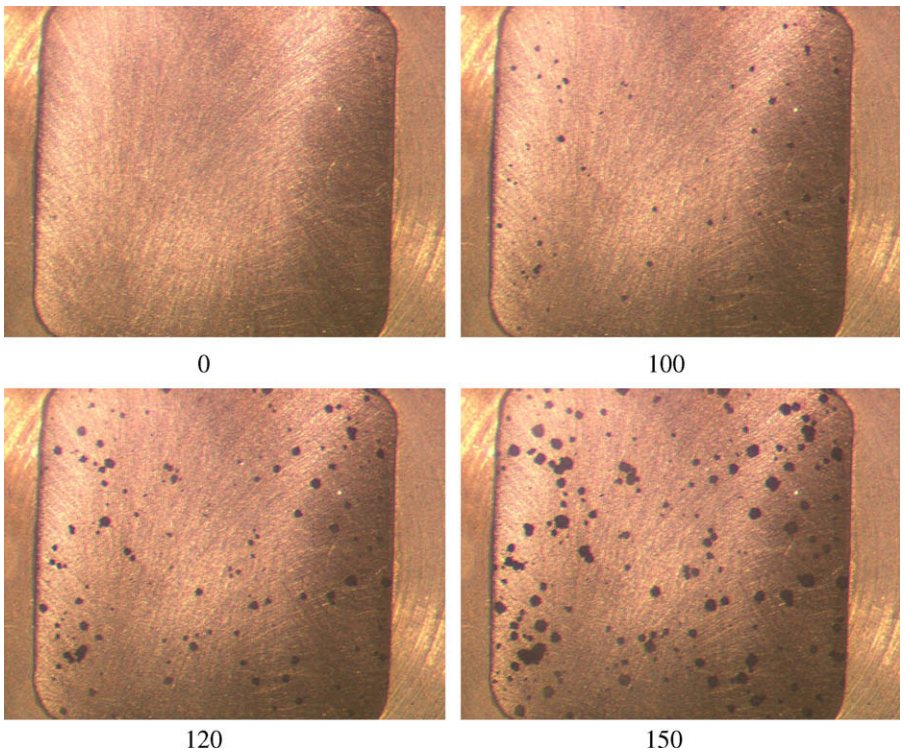

Fig. 3. Sequence of images showing the time-dependent nucleation of hydriding spots from a typical experiment. Initiation time is the time of formation of the first spot. The numbers represent hydrogen exposure times in seconds.

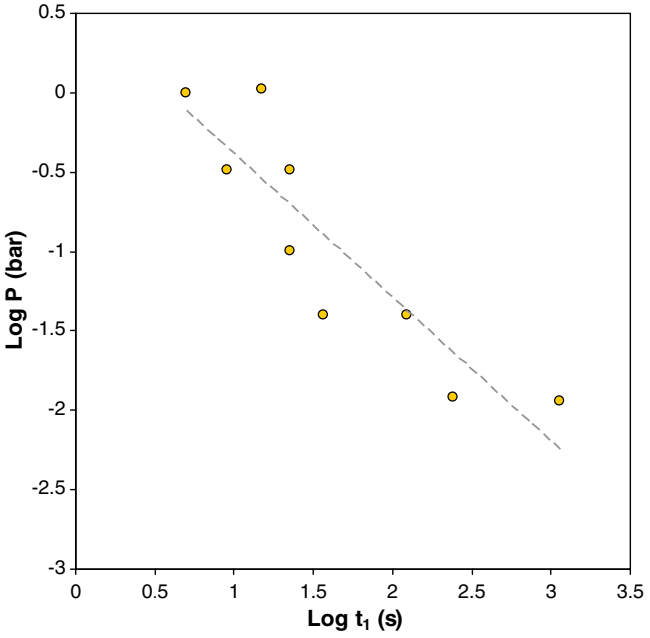

Fig. 4. Log vs. log plot for initiation time (I_t) vs. P. The least squares fit to the data set produces a line with a slope of −0.91, sufficiently close to −1 to suggest that hydriding initiation varies with $1/P$.

sure, i.e. $I_t = k_t/P_{H_2}$. Such an inverse dependence is entirely consistent with a model developed to explain the behaviour of the uranium hydriding reaction in terms of an oxide layer acting as a diffusion barrier to hydrogen transport [10]. The same inverse relationship has also been reported for I_t vs. oxide thickness (under constant pressure conditions) for uranium [22] and zirconium [23].

4. Conclusions

The pressure dependence of the initiation phase of the plutonium hydriding reaction has been determined, at 298 K, over the pressure range 10–1000 mbar. The data show that the initiation time I_t varies inversely with hydrogen pressure; a relationship consistent with a diffusion barrier model of hydride initiation. The low scatter and high degree of reproducibility of the data suggest that the growth of a reproducible oxide layer is a necessary precursor to the quantification of the hydriding initiation parameter I_t.

References

[1] T.H. Allen, J.M. Haschke, Hydride Catalyzed Corrosion of Plutonium: Initiation by Plutonium Monoxide Monohydride, LANL Report LA-13462-MS, 1998.
[2] J.M. Haschke, T.H. Allen, J. Alloys Compd. 320 (2001) 58.
[3] J.M Haschke, J.C Martz, Plutonium Storage. Encyclopaedia of Environmental Analysis and Remediation, John Wiley, 1998. p. 3740.
[4] S.S. Hecker, J.C. Martz (Eds.), Plutonium Aging: From Mystery to Enigma: Proceedings of the International Conference on Ageing Studies and Lifetime Extension of Materials, St. Catherine's College, Oxford, 12–14 July 1999, Kluwer Academic/Plenum Publishing, NY, 2000, p. 23.
[5] J. Bloch, M.H. Mintz, J. Less Common Met. 81 (1981) 301.
[6] J. Bloch, E. Swissa, M.H. Mintz, Z. Phys. Chem. Neue Folge 164 (1989) 1193.
[7] J. Bloch, M.H. Mintz, J. Less Common Met. 166 (1990) 241.
[8] D. Cohen, Y. Zeiri, M.H. Mintz, J. Alloys Compd. 184 (1992) 11.
[9] J. Bloch, M.H. Mintz, IAEC Annual Report, 2001, p. 53.
[10] J. Glascott, AWE Discovery 6 (2003) 16.
[11] J.L. Stakebake, J. Electrochem. Soc. 128 (1981) 2383.
[12] J.L. Stakebake, J. Alloys Compd. 187 (1992) 271.
[13] J. Ogden, C. Alexander, C.A. Colmenares, Isothermal and Isobaric Studies of the Pu–H_2 Reaction, LLNL Report UCRL-84307, 1980.
[14] D.F. Bowersox, The Reaction between Plutonium and Deuterium, Part II. Rate Measurements by Weight Changes, LASL Report LA-6681-MS, 1977.

[15] J.M Haschke, Actinide Hydrides. Topics in Element Chemistry: Synthesis of Lanthanide and Actinide Compounds, Kluwer Academic Publishers, 1991. p. 1.
[16] J.M. Haschke, T.H. Allen, L.A. Morales, Surf. Corros. Chem. Plutonium, Los Alamos Sci. 26 (2000) 252.
[17] I.B. Johns, USAEC MDDC-717, 1944.
[18] F. Brown, H.M. Ockenden, G.A. Welch, J. Chem. Soc. (1955) 3933.
[19] D.F. Bowersox, LASL Report LA-5515-MS, 1974.
[20] K. Terada, R.L. Meisel, M.R. Dringman, J. Nucl. Mater. 30 (1969) 340.
[21] J.M Haschke, in: L.R. Morss, J. Fuger (Eds.), Transuranium Elements a Half Century, ACS, 1992, p. 416 (Chapter 40).
[22] R.M. Harker, J. Alloys Compd. 426 (2006) 106.
[23] Katsumi Une, J. Less Common Met. 57 (1978) 93.